

# Poly(methyl acrylate)/Na-Montmorillonite Intercalated Composites: Preparation and Characterization

Meltem Çelik, Müşerref Önal, Yüksel Sarıkaya

Department of Chemistry, Faculty of Science, Ankara University, 06100 Tandoğan, Ankara, Turkey

Received 13 April 2009; accepted 2 June 2011

DOI 10.1002/app.35033

Published online 22 September 2011 in Wiley Online Library (wileyonlinelibrary.com).

**ABSTRACT:** Poly(methyl acrylate)/Na-montmorillonite intercalated composites were prepared by free-radical polymerization using benzoyl peroxide as a radical initiator in an aqueous medium. XRD patterns confirmed that the increase in interlayer spacing of Na-montmorillonite (Na-MMT) from 1.21 to 1.64 nm supports the intercalation. Although the width of the intercalated, delaminated montmorillonite aggregates are less than 100 nm (as seen in transmission electron microscopy), the prepared samples are members of the intercalated composite group. The samples exhibited better thermal stability than the pure

polymer. Nitrogen adsorption capacity decreased due to the hindering of molecule diffusion and shielding of the intercalated aggregates by the polymer matrix. The decrease in moisture and water uptake of the samples indicated that the hydrophilic nature of montmorillonite changed greatly due to the hydrophobicity with increasing polymer content. © 2011 Wiley Periodicals, Inc. *J Appl Polym Sci* 123: 3662–3667, 2012

**Key words:** composites; clay; poly(methyl acrylate); montmorillonite; free-radical polymerization

## INTRODUCTION

Recently, polymer/clay composites have attracted significant attention due to their excellent physical, mechanical, and thermal properties when compared with the pure polymer.<sup>1–4</sup> Sodium montmorillonite (Na-MMT) is a member of the smectite family, which is a 2 : 1 layered clay mineral that has two tetrahedral sheets sandwiching a central octahedral sheet. The hydrophilic nature, small particle size, and layer-expanding properties of the montmorillonite provide spontaneously homogeneous dispersion in water with a diameter of less than 2  $\mu\text{m}$ . The hydrophilic character of the natural montmorillonite changes partially to the hydrophobic character by the intercalation with monomer molecules before polymerization and insures affinity with polymer chains. The dispersion of clay into a polymer matrix on a nanometer-scale leads to significant improvements in the thermal and mechanical properties, and it also lowers the adsorptive properties of the composites. The improved composites are widely used in areas such as transportation, construction materials, electronics, sporting goods, and some consumer products.<sup>5</sup> Use of clay minerals as inorganic fillers

reduces the cost of inorganic/organic composite products.

Methyl acrylate (MA) is stable in water, easy to synthesize, and is economically efficient; it is also one of the most important vinyl monomers in commercial applications. Poly(methyl acrylate) (PMA), the polymer of methyl acrylate, has low toxicity, is polar and is less expensive than other vinyl polymers. Although PMA has poor thermal and mechanical properties, PMA/Na-MMT composites offer improved thermal stability.

Recently, more attention has been given to polymer/organoclay composites,<sup>6–12</sup> yet studies on polymer/unmodified clay composites are limited.<sup>13–15</sup> Therefore, the aim of this study is to introduce the preparation, characterization, and properties of PMA/Na-MMT composites with radical polymerization.

## EXPERIMENTAL

### Materials

The Na-MMT was obtained by purification from Reşadiye (Tokat/Turkey) bentonite. Cation exchange capacity (CEC) and interlayer spacing ( $d_{001}$ ) of the pure mineral are 1.08 mol  $\text{kg}^{-1}$  and 1.21 nm, respectively. The chemicals used in this study, including methyl acrylate and benzoyl peroxide ( $\text{Bz}_2\text{O}_2$ ), were purchased from Merck Chemical Company. The methyl acrylate monomer was distilled under reduced pressure before use. The free radical initiator,  $\text{Bz}_2\text{O}_2$ , was recrystallized twice from a methanol

Correspondence to: M. Çelik (mecelik@science.ankara.edu.tr).

and chloroform mixture. All other chemicals used were a chemically pure grade.

### Purification of natural bentonite

The natural bentonite was ground and sieved through a 0.074-mm screen. The ground sample was dried at 105°C for 4 h. Na-rich montmorillonite was obtained by the successive decantation from its aqueous suspension.<sup>16</sup>

### Preparation of PMA/Na-MMT composites

First, 1 g Na-MMT was dispersed in 30 mL of distilled water in a 100 mL Pyrex glass tube and was stirred at a rate of 100 rpm in overnight at room temperature for each polymerization. The liquid MA and the aqueous Na-MMT suspension were mixed with the different weight ratios as given in Table I. The Bz<sub>2</sub>O<sub>2</sub> solution in acetone ( $3.0 \times 10^{-3}$  mol/L) was added as 1 mL to the prepared mixtures. The obtained mixtures were polymerized in water bath (Lauda D40 S, Germany) at 85°C for 2 h to synthesize the PMA/Na-MMT composites. The composites were washed thoroughly with acetone to dissolve the remained monomer. The composites were then dried overnight in a vacuum oven at 40°C and weighed. Additional samples were prepared following the same conditions using different quantities of MA. The codes, compositions and polymerization conditions of the samples are listed in Table I.

### Measurements and characterization

The X-ray diffraction (XRD) patterns of the Na-MMT and composites were recorded from random mounts prepared by glass slide method using an Inel Equinox 1000 Powder Diffractometer, operating at 40 kV and 30 mA, using Ni-filtered Co-K $\alpha$  radiation having 0.178901 nm wavelength, at a scanning speed of 2°2 $\theta$  min<sup>-1</sup>.

The morphologies of the Na-MMT and composites coated on gold were examined by a LEO-435 Model scanning electron microscope (SEM). SEM micrographs were taken at 3500 $\times$  magnification. Samples for transmission electron microscopy (TEM) were first embedded in epoxy resin and then ultramicrotomed with a diamond knife at room temperature. Ultrathin sections were transferred from the knife-edge to 300 mesh Cu grids. Transmission electron microscopy micrographs were taken with a LEO-906 E electron microscope at an accelerating voltage of 80 kV. The contrast between the layered clay and polymer phase was sufficient for imaging; therefore, staining was not necessary.

Thermal gravimetric analysis (TGA) and differential thermal analysis (DTA) curves of the samples

**TABLE I**  
Codes and Chemical Compositions of Samples and Polymerization Conditions<sup>a</sup>

Sample code	Monomer content <sup>b</sup> (wt%)	Na-MMT content <sup>c</sup> (wt%)
Na-MMT	–	100.0
PMA/Na-MMT1	20.0	80.0
PMA/Na-MMT2	33.3	66.7
PMA/Na-MMT3	50.0	50.0
PMA/Na-MMT4	60.0	40.0
PMA/Na-MMT5	66.7	33.3
PMA/Na-MMT6	71.4	28.6
Pure PMA	100.0	–

<sup>a</sup> Bz<sub>2</sub>O<sub>2</sub> concentration =  $3.0 \times 10^{-3}$  mol/L, temperature = 85°C, time = 2 h.

<sup>b</sup> Calculated by dividing of the weight of monomer by the weight of (Na-MMT + monomer).

<sup>c</sup> Calculated by dividing of the weight of clay by the weight of (Na-MMT + monomer).

were obtained under air atmosphere using a Shimadzu simultaneous DTA-TG apparatus (DTG-60H Model) thermal analyzer. The temperatures studied ranged from room temperature to 1000°C, and the samples were heated at a rate of 10°C/min.  $\alpha$ -Al<sub>2</sub>O<sub>3</sub> was used as an inert material.

### Nitrogen adsorption

The nitrogen adsorption/desorption isotherms for the samples were obtained at 77 K using a volumetric adsorption instrument, which was fully constructed of Pyrex glass and connected to high vacuum.<sup>17</sup>

### Moisture retention and water uptake measurements

The dried samples were conditioned at 25°C in 100% humidity for 24 h to obtain the moisture retention measurements. The moisture retention percentage was calculated from the difference between the weights of the conditioned and unconditioned samples.<sup>18,19</sup>

The dried samples were weighed and stored in distilled water for 2 h at 25°C. After immersion, the wet samples were wiped using filter paper and reweighed immediately. The water uptake percentage was determined by the difference between the wet and dry weights.<sup>18–20</sup>

## RESULTS AND DISCUSSION

### XRD analysis

Figure 1(a–e) displays the XRD patterns of Na-MMT, which contains opal CT as a nonclay mineral, and PMA/Na-MMT intercalated composites. Bragg's

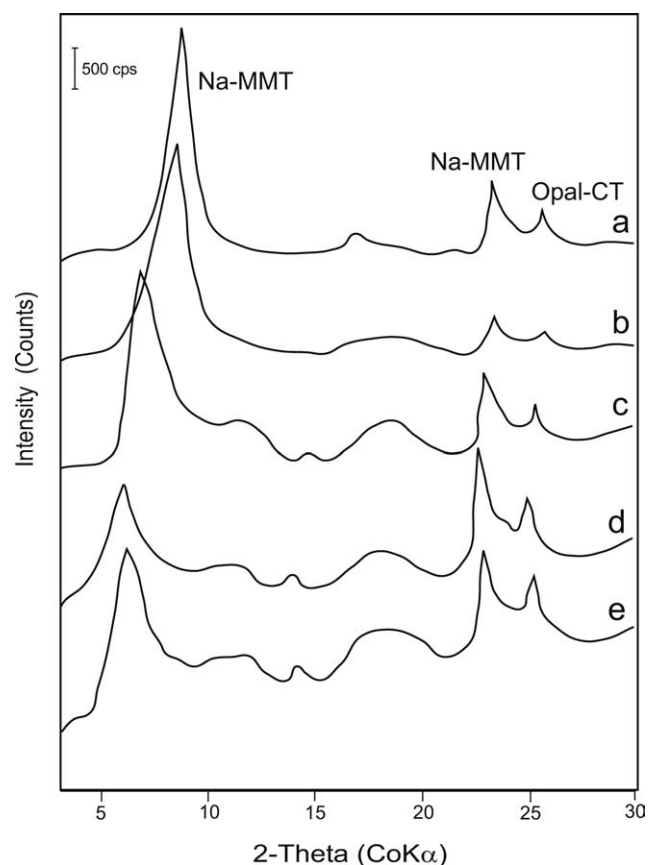


**Figure 1** XRD patterns of Na-MMT and PMA/Na-MMT composites: (a) Na-MMT, (b) PMA/Na-MMT1 (20.0 wt % MA), (c) PMA/Na-MMT2 (33.3 wt % MA), (d) PMA/Na-MMT3 (50.0 wt % MA), (e) PMA/Na-MMT4 (60.0 wt % MA).

equation,  $d = n\lambda/2\sin\theta$ , was used to calculate the interlayer spacings ( $d_{001}$ ) of the samples by using  $\theta$ -values from the XRD patterns. The initial  $d$ -value of Na-MMT was determined to be 1.21 nm. However, the characteristic reflections from the 001 surface in the diffraction patterns of the intercalated composites shifted to a lower  $2\theta$  angle with increasing polymer content (Fig. 1). The peak position and interlayer spacing results are presented in Table II. The maximum value for interlayer spacing was calculated to be 1.64 nm for PMA/Na-MMT3. Because the monomer molecules could penetrate through the interlayer spaces and polymerize without branching, the  $d$ -spacing values of composites are very low. These intercalated but not exfoliated clay particles are dispersed in polymer matrix. The above results were similar to those reported for poly(ethyl acrylate)<sup>1</sup> and polymethacrylamide.<sup>20</sup>

#### Electron microscopy analysis

The SEM images of Na-MMT and PMA/Na-MMT6 composites containing 71.4 wt % MA were given in Figure 2(a,b). These figures showed the difference between surfaces morphologies of the natural clay mineral and one of the composites.

**TABLE II**  
XRD Data for Na-MMT and PMA/Na-MMT Composites

Sample	Peak position $2\theta$ (°)	Interlayer spacing, $d_{001}$ (nm)	Interlayer expansion, $\Delta d_{001}$ (nm)
Na-MMT	8.50	1.21	–
PMA/Na-MMT1	8.36	1.23	0.02
PMA/Na-MMT2	6.68	1.54	0.33
PMA/Na-MMT3	6.26	1.64	0.43
PMA/Na-MMT4	6.29	1.63	0.42

TEM views are necessary to determine the nature of the composite, and it also provides additional information that will aid in the interpretation of the XRD results. TEM micrographs of composites at 8700 and 15,000 magnifications are shown in Figure 3(a,b). The dark bands are due to the intercalated montmorillonite aggregates and the bright regions are from the polymer matrix. The intercalated nano-aggregate is approximately 200 to 400 nm in length and 20 to 40 nm in thickness [Fig. 3(a)]. At higher

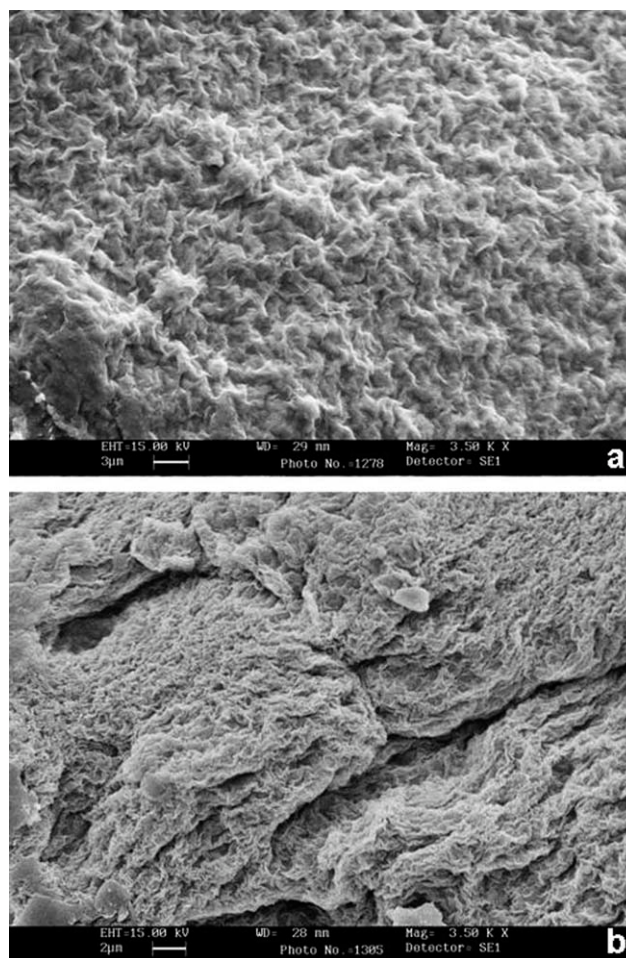


**Figure 2** Scanning electron microscopy micrographs of Na-MMT and PMA/Na-MMT6 composite: (a) Na-MMT, (b) PMA/Na-MMT6 (71.4 wt % MA) at a magnification of  $\times 3500$ .

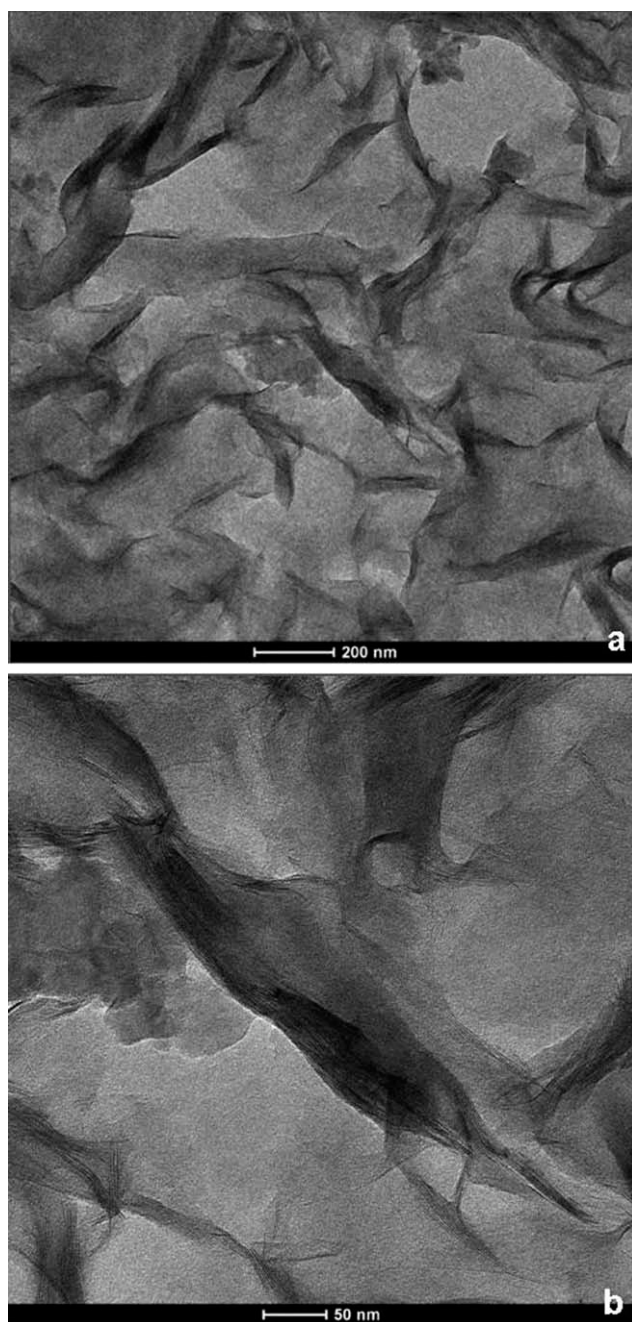


**Figure 3** Transmission electron microscopy micrographs of PMA/Na-MMT3 (50.0 wt % MA) composite. (a) At a magnification of  $\times 8700$ , (b)  $\times 15,000$  magnification.

magnification, larger intercalated layers were also observed. Because the widths of intercalated aggregates are less than 100 nm, the prepared mixtures were considered composites. Similar results were obtained for poly(methyl methacrylate)/clay composite materials.<sup>21–24</sup>

### Thermal analysis

TGA and DTA curves of Na-MMT are given in Figure 4(a) for the temperature range of 25 to 1000°C.

In the curves for Na-MMT, the first endothermic mass loss of 7.8% between 25 and 175°C is due to the dehydration of interparticle water, adsorbed water, and interlayer water. The same sample shows a second endothermic mass loss of 13.0% between 400 and 800°C, which is due to dehydroxylation of the Na-MMT. As expected, the Na-MMT shows high thermal stability.

TGA and DTA curves of pure PMA are given in Figure 4(b) for the temperature range of 25 to 1000°C. The mass loss is 100% for the PMA at 600°C as seen in TGA curve. The endothermic peak between 350 and 450°C with a maximum rate at 415°C in the DTA curve is due to the carbonization

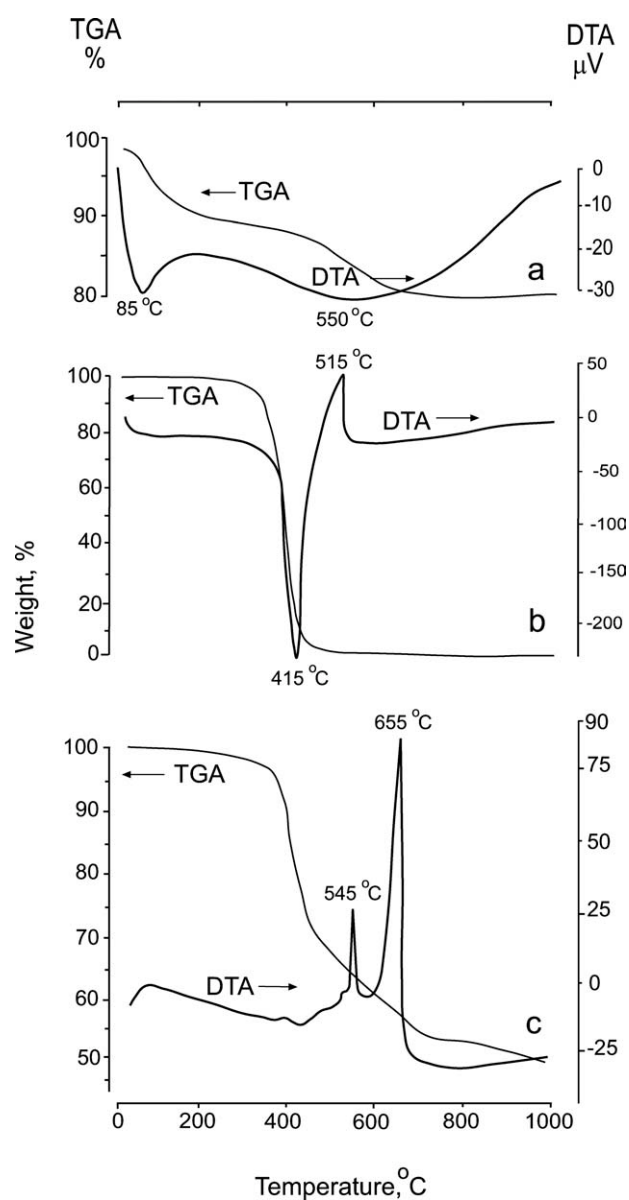


**Figure 4** TGA and DTA curves of Na-MMT, pure PMA, and PMA/Na-MMT3 composite. (a) Na-MMT, (b) pure PMA, (c) PMA/Na-MMT3 (50.0 wt % MA) obtained in air atmosphere.

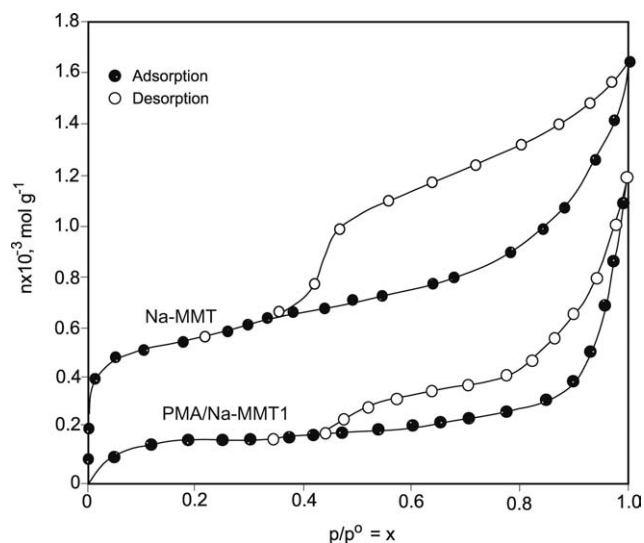


**Figure 5** The adsorption and desorption isotherms of the nitrogen on the Na-MMT and PMA/Na-MMT1 (20.0 wt % MA) composite.

of the PMA and charcoal formation. The exothermic peak between 450 and 550°C with a maximum rate at 515°C is due to the oxidation of charcoal to carbon dioxide.

TGA and DTA curves of PMA/NaMMT3 (50.0 wt % MA) are given in Figure 4(c) for the temperature range of 25 to 1000°C. The mass loss is 45% for the PMA/Na-MMT3 composite at 1000°C as seen in TGA curve. The wide endothermic peak between 100 and 515°C is originated from slow carbonization of the polymer in the composite. The first exothermic peak in the range of 515 to 570°C with a maximum rate at 545°C belongs to the oxidation of charcoal coming probably from the decomposition of the remained bulk polymer. The second exothermic peak with high intensity in the interval of 570 to 675°C with a maximum rate at 655°C is due to the oxidation of charcoal coming probably from polymer in the composite. The composite is thermally more stable than the pure polymer. This conclusion is consistent with other reported results.<sup>22–26</sup>

### Adsorptive properties

The adsorption/desorption isotherms of the nitrogen on the Na-MMT and PMAA/Na-MMT1 composite are presented in Figure 5. Here,  $p$  represents the adsorption equilibrium pressure,  $p^0$  represents the saturated vapor pressure of liquid nitrogen, and  $p/p^0 \equiv x$  represents the relative equilibrium pressure. The adsorption capacity, defined as  $n$  ( $\text{mol g}^{-1}$ ), is the molar quantity of nitrogen adsorbed by 1 g of sample. As was expected, the Na-MMT showed the higher adsorption capacity when compared with the PMA/Na-MMT1 composite.

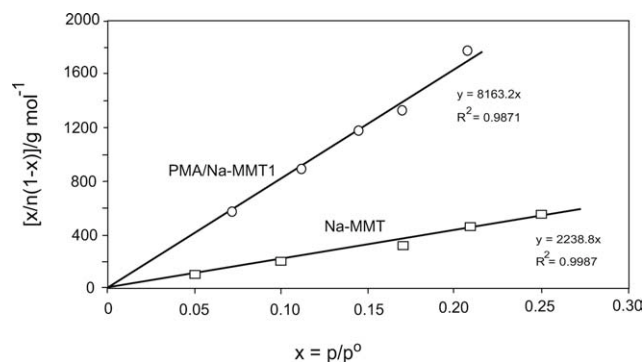


**Figure 6** The Brunauer-Emmett-Teller (BET) straight line of the Na-MMT and PMAA/Na-MMT1 composite.

The specific surface areas ( $S_{\text{BET}}$ ) for Na-MMT and PMAA/Na-MMT1 composite were determined from the Brunauer-Emmett-Teller (BET) plots (Fig. 6), which were drawn using  $\text{N}_2$  adsorption data.<sup>27–29</sup> The specific micropore volumes ( $V$ ) were calculated from the desorption isotherms at the  $p/p^0 = 0.96$ .<sup>30</sup> The  $S_{\text{BET}}$  and  $V$  values were given in Table III.

It was observed that while the specific surface area and micro-mesopore volume of Na-MMT were  $43.56 \text{ m}^2 \text{ g}^{-1}$  and  $0.054 \text{ cm}^3 \text{ g}^{-1}$ , these values drastically decreased to  $11.95 \text{ m}^2 \text{ g}^{-1}$  and  $0.032 \text{ cm}^3 \text{ g}^{-1}$  for PMA/Na-MMT1 containing 20.0 wt % MA. A potential explanation suggests that the pores were covered or filled by PMA.<sup>4,18</sup>

### Moisture retention and water uptake capacities

The moisture retained and water uptake values of Na-MMT and PMA/Na-MMT composites are shown in Table IV. It was observed that moisture retention gradually decreased, while water uptake of the composites sharply decreased with the increase of monomer content.

The decreases in moisture retention and water uptake can be attributed to the hydrophobic character of the PMA and the hydrophilicity of Na-MMT became more organophilic in nature. In other words, the decrease in the moisture retention and water uptake observed in the composites PMA/Na-MMT 1 to 6 also could be related to the decrease of the Na-MMT content, which is reduced from 80 wt % (PMA/Na-MMT1) to 28.6 wt % (PMA/Na-MMT6),

**TABLE III**  
The Specific Surface Areas ( $S_{\text{BET}}$ ) and Specific Micro-Mesopore Volumes ( $V$ ) of the Na-MMT and PMA/Na-MMT1 Composite

Sample	$S_{\text{BET}}$ ( $\text{m}^2 \text{ g}^{-1}$ )	$V$ ( $\text{cm}^3 \text{ g}^{-1}$ )
Na-MMT	43.56	0.054
PMA/Na-MMT1	11.95	0.032

**TABLE IV**  
**The Moisture Retain and Water Uptake Values of Na-MMT, Pure PMA, and PMA/Na-MMT Composites<sup>a</sup>**

Sample	Moisture retain (%)	Water uptake(%)
Na-MMT	39.33	342.39
Pure PMA	0.44	4.02
PMA/Na-MMT1	34.35	105.88
PMA/Na-MMT2	19.28	54.94
PMA/Na-MMT3	17.83	49.78
PMA/Na-MMT4	11.73	6.03
PMA/Na-MMT5	8.98	5.26
PMA/Na-MMT6	8.79	3.65

<sup>a</sup> At room temperature.

since the sodium MMT presents a high hydrophilic character. The decrease in water uptake meant that the material had more stable properties, which is useful in practical applications.<sup>29</sup> Finally, water resistance of these composites could be greatly improved.<sup>30,31</sup>

## CONCLUSIONS

Poly(methyl acrylate)/Na-MMT intercalated composites were successfully prepared using free-radical polymerization. Their thermal, adsorptive, moisture-retaining, and water-uptaking properties were investigated. It was observed that the intercalation increased with increasing polymer content and intercalated aggregates were formed in the polymer matrix. The composites exhibited better thermal stability than the pure PMA. Porosity, surface area, moisture retention and water uptake of Na-MMT decreased by increasing the polymer content in the prepared composites.

The authors thank Earth Sciences Application and Research Center (YEBİM) of Ankara University (Turkey) for XRD analysis support.

## References

- Tong, X.; Zhao, H.; Tang, T.; Feng, Z.; Huang, B. *J Polym Sci Part A: Polym Chem* 2002, 40, 1706.
- Shen, Z.; Simon, G. P.; Cheng, Y. B. *J Appl Polym Sci* 2004, 92, 2101.
- Mert, M.; Yilmazer, U. *J Appl Polym Sci* 2008, 108, 3890.
- Çelik, M.; Önal, M. *JMS Pure Appl Chem* 2006, 43, 933.
- Fu, X.; Qutubuddin, S. *Polymer* 2001, 42, 807.
- Wang, H. W.; Chang, K. C.; Yeh, J. M.; Liou, S. J. *J Appl Polym Sci* 2004, 91, 1368.
- Basara, C.; Yilmazer, U.; Bayram, G. *J Appl Polym Sci* 2005, 98, 1081.
- Cheng-Yang, Y. W.; Yang, H. C.; Li, G. J.; Li, Y. K. *J Polym Res* 2005, 11, 275.
- Tiwari, R. R.; Natarajan, U. *Polym Int* 2008, 57, 738.
- Huskic, M.; Zigon, M. *Eur Polym Mater* 2007, 43, 4891.
- Shi, X.; Gan, Z. *Eur Polym Mater* 2007, 43, 4852.
- Kumar, S.; Jog, J. P.; Natarajan, U. *J Appl Polym Sci* 2003, 89, 1186.
- Leitea, A. M. D.; Araujoa, E. M.; Paza, R. A.; Pereira, O. D.; Liraa, H. L.; Itob, E. N. *Mater Res* 2009, 12, 165.
- Dong, W.; Zhang, X.; Liu, Y.; Gui, H.; Wang, Q.; Gao, J.; Song, Z.; Lai, J.; Huang, F.; Qiao, J. *Eur Polym Mater* 2006, 42, 2515.
- Tarapow, J. A.; Bernal, C. R.; Alvarez, V. A. *J Appl Polym Sci* 2009, 111, 768.
- Önal, M.; Sarıkaya, Y.; Alemdaroğlu, T.; Bozdoğan, İ. *Turk J Chem* 2003, 27, 683.
- Önal, M.; Sarıkaya, Y.; Alemdaroğlu, T. *Turk J Chem* 2001, 25, 241.
- Çelik, M.; Önal, M. *J Appl Polym Sci* 2004, 94, 1532.
- Çelik, M. *J Polym Res* 2006, 13, 427.
- Önal, M.; Çelik, M. *Mater Lett* 2006, 60, 48.
- Kim, S. S.; Park, T. S.; Shin, B. C.; Kim, Y. B. *J Appl Polym Sci* 2005, 97, 2340.
- Huang, X.; Brittain, W. J. *Macromolecules* 2001, 34, 3255.
- Li, Y.; Zhao, B.; Xie, S.; Zhang, S. *Polym Int* 2003, 52, 892.
- Zhu, J.; Start, P.; Mauritz, K. A.; Wilkie, C. A. *Polym Degrad Stab* 2002, 77, 253.
- Nikolaidis, A. K.; Achilias, D. S.; Karayannidis, G. P. *Ind Eng Chem Res* 2011, 50, 571.
- Çelik, M.; Önal, M. *J Polym Res* 2007, 14, 313.
- Brunauer, S.; Emmett, P. H.; Teller, E. *J Am Chem Soc* 1938, 60, 309.
- Sarıkaya, Y.; Alemdaroğlu, T.; Önal, M. *J Eur Ceram Soc* 2002, 22, 305.
- Han, B.; Cheng, A.; Ji, G.; Wu, S.; Shen, J. *J Appl Polym Sci* 2004, 91, 2536.
- Low, H. Y.; Liu, T. X.; Loh, W. W. *Polym Int* 2004, 53, 1973.
- Keleş H.; Çelik, M.; Saçak, M.; Aksu, L. *J Appl Polym Sci* 1999, 74, 1547.